Effects of Unequal Diffusion Coefficients and Coupled Chemical Equilibria on Square Wave Voltammetry at Disc and Hemispherical Microelectrodes

J. M. Olmos, A. Molina*, E. Laborda, F. Martínez-Ortiz

Departamento de Química Física, Facultad de Química, Regional Campus of International Excellence "Campus Mare Nostrum", Universidad de Murcia, 30100 Murcia, Spain

* Corresponding author:

Tel: +34 868 88 7524

Fax: +34 868 88 4148

Email: amolina@um.es

Abstract

Square wave voltammetry (SWV) at disc and hemispherical microelectrodes is studied when the electroactive species show different diffusivities and/or take part in chemical equilibria in solution, under both transient and steady state conditions. Despite the use of microelectrodes, experiments in pulse techniques such as SWV frequently correspond to transient conditions since the pulse duration are typically very short (<100ms, f>5Hz). As will be shown, under such conditions the case of unequal diffusion coefficients gives rise to a complex behaviour of the SWV peak, the features of which deviate from the theory and criteria already established under the assumption of equal diffusion coefficients. Also, the theoretical treatment is notably more difficult and no analytical solution has been deduced for multipulse techniques.

The effects of coupled chemical equilibria and, particularly, of unequal diffusion coefficients on SWV will be described in depth as a function of the electrode size and shape and they will be compared with those observed in differential double pulse voltammetry (DDPV). The main discrepancies in the peak height, width and position with respect to the case of equal diffusion coefficients will be studied. Also, appropriate methodologies and experimental conditions will be discussed for the determination of, formal potentials and equilibrium constants.

Keywords: Square wave voltammetry; Microelectrodes; Unequal diffusion coefficients; Coupled chemical equilibria; Differential double pulse voltammetry

1. INTRODUCTION

Two difficulties that may arise in the modelling and interpretation of electrochemical experiments are differences between the diffusivities of the electroactive species as well as the incidence of homogeneous chemical processes coupled to the electron transfer. Thus, one and even two orders of magnitude differences in the diffusion coefficients have been reported between free species and species associated with large (bio)molecules or nanoparticles [1-5]. Examples of coupled chemical processes commonly-encountered in electrochemical studies include structural rearrangements [6], protonations [7, 8], ion pairing [9, 10] and complexations [11, 12].

As an example of the situations above mentioned, in this work the case of the four-member square scheme given in Scheme I is tackled at disc and spherical electrodes of any size without any restrictions in the values of the diffusion coefficients of the different species:

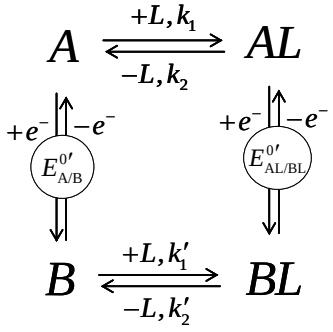

Scheme I

The results obtained are applicable to a range of experimental systems where coupled chemical equilibria involve the reactant species ($C_{eq}E_{rev}$-like reactions), the product species ($E_{rev}C_{eq}$-like reactions), both electroactive species (square scheme) or none of them (E mechanism). Moreover, the theory reported in this paper can be applied to the study of ion transfer processes at liquid|liquid macrointerfases [13, 14] and, as a first approach, at microinterfaces supported at micropores and microholes [15, 16]. Note that

notable differences between the diffusion coefficients of the target ion in each phase are frequently observed, especially when one of them is a liquid membrane [17] or room temperature ionic liquids [18-21] such that the results here reported are of interest in this field.

The effect of a significant change in the effective diffusion coefficient of the electrolysed species on square wave voltammetry (SWV) will be deeply studied at disc and hemispherical electrodes and compared with the behaviour predicted in differential double pulse voltammetry (DDPV). Particular attention will be paid to electrodes of micrometer size, which are commonly employed in order to reduce capacitive effects and to perform measurements in small volumes and resistive media [22], and where the use of differential techniques is recommended with the aim of obtaining well-defined, peak-shaped signals of high sensitivity and reduced background effects [23-27].

At microelectrodes, when the values of the effective diffusion coefficients are different, the surface concentration of the electroactive species are time-dependent even in the case of reversible electrode [28]. As a consequence, the theoretical description of the system is much more difficult. Thus, whereas simple, analytical expressions can be deduced for SWV whatever the electrode size and shape when the effective diffusion coefficients are [9, 23, 24], the use of numerical treatments is mostly necessary when the values of the diffusion coefficients differ significantly.

The complications above-mentioned affects the experimental signal, the electrochemical response showing some important peculiarities that are not predicted when equal diffusion coefficients are assumed [23-25, 27, 29]. Thus, as will be shown, both the position and magnitude of the peaks are affected by the time-scale of the experiment and by the electrode size. On the one hand, this makes the interpretation and quantitative analysis of experiments more challenging, for which mathematical

solutions and qualitative criteria will be given here. On the other hand, the use of microelectrodes enables us to gain further insight into the system since simultaneous determination of the formal potential and diffusion coefficients of reactant and product species is feasible from SWV experiments with only one (disc or hemispherical) microelectrode even when the product species are not initially present, unlike what happens when macroelectrodes or electrodes of submicrometric size are employed.

Other electrochemical techniques have also been considered to determine diffusion coefficients, such as double pulse chronoamperometry and reverse pulse voltammetry [30-35]. They show some advantages with respect to the determination from the peak current in SWV, DDPV [36] or cyclic voltammetry (CV) [37, 38], although the extraction of the formal potential is more difficult and less accurate given the non-peak shaped signal. Moreover, CV is more affected by capacitive and background effects than the subtractive techniques SWV and DDPV. Normal Pulse Voltammetry (NPV) and Derivative Voltammetry (DV) have also been considered to obtain diffusion coefficients [28]. In both techniques, the extraction of the values of the diffusion coefficients is based on the position of the current-potential curves, instead of on their magnitude as in CV, SWV and DDPV. This may compromise the accuracy of the study since the NPV response is sigmoidal and the experimental peak recorded in DV can show a low signal to noise ratio after the differentiation of the digitally acquired NPV curve [39].

2. THEORY

In order to model the electrochemical response of the system given in Scheme I, species L is assumed to be initially present in large excess with respect to the electroactive species such that its concentration does not change significantly upon the application of a voltammetric perturbation (*i.e.*, $c_{\mathrm{L}}(q,t) \approx c_{\mathrm{L}}^{*}$). Also, the homogeneous chemical processes are supposed to be very fast so that chemical equilibrium conditions apply at any position in solution (q) and time of the experiment (t):

$$\begin{aligned} \frac{c_{\mathrm{AL}}(q,t)}{c_{\mathrm{A}}(q,t)} &= K = \frac{k_1 c_{\mathrm{L}}^{*}}{k_2} \\ \frac{c_{\mathrm{BL}}(q,t)}{c_{\mathrm{B}}(q,t)} &= K' = \frac{k_1' c_{\mathrm{L}}^{*}}{k_2'} \end{aligned} \tag{1}$$

where k_1, k_1' and k_2, k_2' are the forward and backward rate constants of the homogeneous chemical reactions (see Scheme 1) and K and K' are the *effective* equilibrium constants, which relate to the formal potentials as follows:

$$\frac{K}{K'} = \exp\left(\frac{F}{RT}\left(E_{\mathrm{A/B}}^{0'} - E_{\mathrm{AL/BL}}^{0'} \right) \right) \tag{2}$$

with $E_{\mathrm{A/B}}^{0'}$ and $E_{\mathrm{AL/BL}}^{0'}$ being the formal potentials of the redox couples A/B and AL/BL, respectively.

Taking into account the above considerations, the problem corresponding to the variation of the species concentrations when applying a voltammetric perturbation $E(t)$ can be reduced to the following differential equation [9, 28] system:

$$\left.\begin{aligned} \frac{\partial c_{\mathrm{AT}}(q,t)}{\partial t} &= D_{\mathrm{eff}} \nabla^2 c_{\mathrm{AT}}(q,t) \\ \frac{\partial c_{\mathrm{BT}}(q,t)}{\partial t} &= D_{\mathrm{eff}}' \nabla^2 c_{\mathrm{BT}}(q,t) \end{aligned}\right\} \tag{3}$$

where $c_{i\mathrm{T}}$ ($i \equiv$A,B) are the total concentrations of the oxidized and reduced species:

$$\left.\begin{aligned} c_{\mathrm{AT}}(q,t) &= c_{\mathrm{A}}(q,t) + c_{\mathrm{AL}}(q,t) \\ c_{\mathrm{BT}}(q,t) &= c_{\mathrm{B}}(q,t) + c_{\mathrm{BL}}(q,t) \end{aligned}\right\} \tag{4}$$

the effective diffusion coefficients, D_{eff} and D'_{eff}, are defined as

$$\begin{aligned} D_{\mathrm{eff}} &= \frac{D_{\mathrm{A}} + KD_{\mathrm{AL}}}{1+K} \\ D'_{\mathrm{eff}} &= \frac{D_{\mathrm{B}} + K'D_{\mathrm{BL}}}{1+K'} \end{aligned} \tag{5}$$

and ∇^2 is the Laplacian operator of diffusion [40]

$$\begin{aligned} \nabla^2_{\mathrm{sph}} &= \frac{\partial^2}{\partial r^2} + \frac{2}{r}\frac{\partial}{\partial r} \\ \nabla^2_{\mathrm{disc}} &= \frac{\partial^2}{\partial r^2} + \frac{1}{r}\frac{\partial}{\partial r} + \frac{\partial^2}{\partial z^2} \end{aligned} \tag{6}$$

The boundary value problem in terms of c_{iT} is given by

$$\left.\begin{aligned} q \geq q_{\mathrm{s}}, t = 0 \\ q \to \infty, t \geq 0 \end{aligned}\right\} \qquad c_{\mathrm{AT}} = c^*_{\mathrm{AT}} \quad ; \quad c_{\mathrm{BT}} = 0 \tag{7}$$

$$q = q_{\mathrm{s}}, t > 0\} \qquad \gamma^2 \left(\frac{\partial c_{\mathrm{AT}}(q,t)}{\partial q_{\mathrm{N}}}\right)_{q=q_{\mathrm{s}}} = -\left(\frac{\partial c_{\mathrm{BT}}(q,t)}{\partial q_{\mathrm{N}}}\right)_{q=q_{\mathrm{s}}} \tag{8}$$

$$c_{\mathrm{AT}}(q_{\mathrm{s}},t) = c_{\mathrm{BT}}(q_{\mathrm{s}},t)\omega\,\mathrm{e}^{\eta} \tag{9}$$

where it has been assumed that only species A and AL are initially present and q_{s} corresponds to the spatial coordinates at the electrode surface, q_{N} is the coordinate normal to the surface, c^*_{AT} the total initial concentration of oxidized species, and

$$\gamma = \sqrt{\frac{D_{\mathrm{eff}}}{D'_{\mathrm{eff}}}} \tag{10}$$

$$\omega = \frac{1+K}{1+K'} \tag{11}$$

$$\eta = \frac{F}{RT}\left(E - E^{0'}_{\mathrm{A/B}}\right) \tag{12}$$

It is important to highlight that from Eq. (9) it is possible to define the *apparent* formal potential as follows:

$$E_{\text{app}}^{0'} = E_{\text{A/B}}^{0'} + \frac{RT}{F}\ln\left(\frac{1}{\omega}\right) \tag{13}$$

such that the problem given by Eqs. (3) and (7)-(9) is formally identical to that of a reversible E mechanism of the "pseudo" redox couple AT/BT that is characterized by $E_{\text{app}}^{0'}$ and the diffusion coefficients D_{eff} and D'_{eff}. This conclusion is also reached when the possible homogeneous cross reaction between species in Scheme I is considered:

$$\text{A+BL} \rightleftharpoons \text{B+AL} \tag{14}$$

given that this reaction is chemically dependent on the equilibria A/AL and B/BL.

2.1. *Equal* (*effective*) *diffusion coefficients*

When equal (effective) diffusion coefficients can be assumed, $D_{\text{eff}} = D'_{\text{eff}} = D$, which is reasonable for many processes in conventional solvents, it has been demonstrated that a general analytical expression can be derived for the response at disc and spherical electrodes of any radius r_0 when an arbitrary sequence of *p* potential pulses is applied [9] ($E_1, E_2 ... E_p$):

$$I_{\text{p}}^{\gamma=1} = FA_{\text{G}}Dc_{\text{AT}}^{*}\sum_{m=1}^{\text{p}} Z_{\text{m}}\, f_{\text{G}}\left(r_0, t_{\text{mp}}\right) \tag{15}$$

where A_{G} is the electrode area, Z_{m} is a function of the applied potential:

$$\begin{aligned} Z_1 &= \frac{1}{1+\omega\,\text{e}^{\eta_1}} \\ Z_{\text{m}} &= \frac{1}{1+\omega\,\text{e}^{\eta_{\text{m}}}} - \frac{1}{1+\omega\,\text{e}^{\eta_{\text{m-1}}}} \quad m \geq 2 \end{aligned} \tag{16}$$

and $f_{\text{G}}\left(r_0, t_{\text{mp}}\right)$ is a function of time and the electrode geometry 'G':

$$f_{macro}\left(t_{\mathrm{mp}}\right)=\frac{1}{\sqrt{\pi D t_{\mathrm{mp}}}}$$

$$f_{\mathrm{sph}}\left(r_0,t_{\mathrm{mp}}\right)=\left(\frac{1}{r_0}+\frac{1}{\sqrt{\pi D t_{\mathrm{mp}}}}\right) \tag{17}$$

$$f_{\mathrm{disc}}\left(r_0,t_{\mathrm{mp}}\right)=\frac{4}{\pi r_0}\left(0.7854+0.44315\frac{r_0}{\sqrt{D t_{\mathrm{mp}}}}+0.2146\exp\left(-0.39115\frac{r_0}{\sqrt{D t_{\mathrm{mp}}}}\right)\right)$$

where $t_{\mathrm{mp}}=t_{\mathrm{p}}+\sum_{i=m}^{p-1}\tau_{\mathrm{i}}$ with τ_{i} being the duration of each potential pulse and $0\le t_p\le\tau_p$.

From Eq. (15), the signal in any multipulse technique can be calculated by specifying the form of the potential-time perturbation. The waveform in cyclic square wave voltammetry can be described as (Figure 1A) [41]:

$$\left.\begin{array}{ll} E_{\mathrm{p}}=E_{\mathrm{initial}}+\left[Int\left(\frac{p+1}{2}\right)-1\right]E_{\mathrm{s}}+\left(-1\right)^{\mathrm{p}}E_{\mathrm{SW}};\quad p=1,\ 2,\ \ldots,N/2 & \text{forward scan} \\ E_{\mathrm{p}}=E_{\mathrm{N-p+1}};\quad p=\left(N/2\right)+1,\ \ldots,N & \text{reverse scan} \end{array}\right\} \tag{18}$$

where E_{s} is the potential step in the staircase, E_{SW} the square wave amplitude, N the total number of pulses applied and $Int(x)$ the integer part of the argument x (see Fig.1B). The SWV response is obtained from the difference between the current corresponding to a pulse with odd index (I_{f}) and that of the consecutive pulse with even index (I_{b}) that comprise the cycle c:

$$\Delta I_{\mathrm{SWV}}=I_{2c-1}-I_{2c}=I_{\mathrm{f}}-I_{\mathrm{b}}\quad;\quad c=1,2...,N/2 \tag{19}$$

so that from (15) one can obtains that:

$$\Delta I_{\mathrm{SWV}}^{\gamma=1}=FA_{\mathrm{G}}Dc_{\mathrm{AT}}^{*}\left[\sum_{m=1}^{2c-1}Z_m f_G\left(q_G,\left(2c-m\right)\tau\right)-\sum_{m=1}^{2c}Z_m f_G\left(q_G,\left(2c-m+1\right)\tau\right)\right] \tag{20}$$

where $c=1,2...,N/2$ and τ is the duration of each potential pulse such that the frequency value is given by: $f=1/2\tau$.

As shown in Figure 1B, in the DDPV method independent double potential pulses $\{E_1, E_2 = E_1 + \Delta E\}$ are applied, the initial conditions being restored afterwards. The current is sampled at the end of the first ($I_1(\tau_1)$) and second ($I_2(\tau_1 + \tau_2)$) pulses and the DDPV curve is calculated from $\Delta I_{\mathrm{DDPV}} = I_2(\tau_1 + \tau_2) - I_1(\tau_1)$. Taking into account that in DDPV the first pulse is typically much longer than the second one, $\tau_1 \geq 50\,\tau_2$, the expression for the response at any electrode geometry simplifies to:

$$\Delta I_{\mathrm{DDPV}}^{\gamma=1} = FA_{\mathrm{G}} D c_{\mathrm{AT}}^{*} \frac{\omega\left(\mathrm{e}^{\eta_1} - \mathrm{e}^{\eta_2}\right)}{\left(1+\omega\,\mathrm{e}^{\eta_1}\right)\left(1+\omega\,\mathrm{e}^{\eta_2}\right)} f_G(r_0, \tau_2) \tag{21}$$

2.2. *Unequal (effective) diffusion coefficients*

There are some experimental systems of notable interest where the assumption of equal effective diffusion coefficients may not be [1-5, 17-21] adequate. Depending on the electrode geometry, this may introduce higher complexity in the resolution of the mathematical problem.

When $D_{\mathrm{eff}} \neq D'_{\mathrm{eff}}$, the surface concentrations of the electroactive species are time-independent at *macroelectrodes* ($r_0 \to \infty$) and so the superposition principle still applies. Therefore, the general equations presented above for $\gamma = 1$ are applicable by changing e^{η_m} by $\gamma\mathrm{e}^{\eta_m}$. The case of submicrometric-sized electrodes ($r_0 \to 0$) is also easy to tackle for $D_{\mathrm{eff}} \neq D'_{\mathrm{eff}}$ given that steady state conditions are reached and the response at each potential pulse is independent of the previous ones. Taking this into account, the SWV steady state response at (hemi)spherical and disc submicrometric-sized electrodes can be written as [22, 42]:

$$\Delta I_{\mathrm{SWV}}^{\mathrm{sph\ UME}} \to \frac{\mathrm{FA}c_{\mathrm{AT}}^{*} D_{\mathrm{eff}}}{r_0} \frac{\gamma^2\omega\left(\mathrm{e}^{\eta_{2c}} - \mathrm{e}^{\eta_{2c-1}}\right)}{\left(1+\gamma^2\omega\,\mathrm{e}^{\eta_{2c-1}}\right)\left(1+\gamma^2\omega\,\mathrm{e}^{\eta_{2c}}\right)} \tag{22}$$

$$\Delta I_{\mathrm{SWV}}^{\mathrm{disc\ UME}} \to 4\,\mathrm{F} c_{\mathrm{AT}}^{*} D_{\mathrm{eff}}\, r_0 \frac{\gamma^2 \omega \left(\mathrm{e}^{\eta_{2c}} - \mathrm{e}^{\eta_{2c-1}} \right)}{\left(1 + \gamma^2 \omega\, \mathrm{e}^{\eta_{2c\text{-}1}}\right)\left(1 + \gamma^2 \omega\, \mathrm{e}^{\eta_{2c}}\right)} \tag{23}$$

which coincides with the expressions obtained for DDPV with $|\Delta E| = 2|E_{\mathrm{SW}}|$ (see Figure 1).

2.2.1. *Microelectrodes under transient conditions*

The problem and electrochemical response at microelectrodes under transient conditions gets notably difficult when the effective diffusion coefficients are unequal. A rigorous analytical solution has been obtained for the DDPV response at spherical electrodes of any size by using a modification of Koutecký´s dimensionless parameters method [36]. For SWV (and for DDPV at disc microelectrodes), finite difference numerical methods implemented in homemade programs have been used in this work. Regarding electrodes of spherical geometry, an exponentially expanding grid has been used for the spatial discretization with asymmetric 4-point approximation of the derivatives and the EXTRAP4 extrapolation algorithm for time integration [43]. In the case of disc microelectrodes, the DDPV and SWV responses have been simulated by making use of the alternating direction implicit (ADI) approach with an spatial grid in the (*r*,*z*)-domain with high density of nodes at the electrode surface and edge, 3-point difference approximations for the spatial derivatives and a regular time grid [44].

3. RESULTS AND DISCUSSION

As mentioned in Section 2, the influence of coupled chemical equilibria on the voltammograms results in the change of the *apparent* formal potential of the redox couple according to Eq. (13). This effect is parameterised through the value of ω (Eq. (11)) such that large ω-values are associated with situations where the complex of species A is more stable than that of species B, while the opposite corresponds to small values of ω. Consequently, the increase of ω leads to the shift of the voltammogram towards more negative potentials as a result of the hindering of the electroreduction of the oxidized species [9, 36] species, which can be employed for the determination of the equilibrium constants from experimental values of $E_{\text{app}}^{0'}$ obtained at different concentrations of species L [9]. On the other hand, the peak current and width are insensitive to the ω-value. Therefore, for the sake of generality, hereinafter the potential-*axis* in the figures will be referred to the value of the *apparent* formal potential $E_{\text{app}}^{0'}$.

Next, the influence of unequal diffusion coefficients on the SWV response will be analyzed in depth, describing how it affects the magnitude and shape of the peaks as well as their dependence with the experimental variables such as the electrode geometry, the time-scale of the experiments and the pulse amplitude. In Figure 2, one can see the influence of the ratio between the effective diffusion coefficients $\left(\gamma = \sqrt{D_{\text{eff}} / D'_{\text{eff}}}\right)$ at spherical and disc electrodes of different radii. Regardless of the electrode size and geometry, both in SWV and DDPV the position of the peak is dependent on γ and it shifts towards more negative potentials as γ increases. However, the peak current is only affected by D'_{eff} at medium-size microelectrodes (Fig. 2B) such that the peak height increases with γ (that is, as D'_{eff} decreases). This behaviour has

been verified for other typical values of SWV and DDPV amplitudes (not shown). On the other hand, neither at planar electrodes (Fig. 2A) nor at ultramicroelectrodes (UMEs, Fig. 2C) is ΔI_{peak} sensitive to D'_{eff}. Therefore, an appropriate microelectrode size must be selected in order to determine γ from the peak height.

At ultramicroelectrodes (Fig. 2C), the SWV and DDPV curves with $E_{\text{SW}} = |\Delta E| / 2$ are equivalent since steady state conditions hold and the system loses the 'memory' of previous pulses. Note that the current density at disc microelectrodes is larger than at spherical ones. The following ratio is found under steady state conditions:

$$\frac{\Delta I_{\text{peak}}^{\text{disc UME}} / \text{A}_{\text{disc}}}{\Delta I_{\text{peak}}^{\text{sph UME}} / \text{A}_{\text{sph}}} = \frac{4}{\pi} \frac{r_{\text{s}}}{r_{\text{d}}} \tag{24}$$

where r_{s} and r_{d} are the radius of the (hemi)spherical and disc electrodes, respectively. Obviously, the same response is obtained at both geometries when the electrode size is sufficiently large (Fig. 2A) since diffusion is linear.

With respect to the position of the voltammograms, it is observed that the peak potential (E_{peak}) is not significantly affected by the electrode geometry though it depends on the time-scale of the experiment and the electrode size when the (effective) diffusion coefficients differ. A comparison between the peak potentials in SWV $\left(E_{\text{peak}}^{\text{SWV}}\right)$ and DDPV $\left(E_{\text{peak}}^{\text{DDPV}}\right)$ and the half-wave potential ($E_{1/2}$) is shown in Figure 3 for three different γ-values (10, 1 and 0.1). The values of the peak potential coincide with $E_{1/2}$ at macroelectrodes ($\sigma >> 1$; $\sigma^{\text{SWV}} = r_0^2 / D_{\text{eff}}\tau$, $\sigma^{\text{DDPV}} = r_0^2 / D_{\text{eff}}\tau_2$), where the following expression holds [22]:

$$E_{\text{peak}}^{\text{SWV,plane}} = E_{\text{peak}}^{\text{DDPV,plane}} = E_{1/2}^{\text{plane}} = E_{\text{app}}^{0'} + \frac{RT}{F} \ln\left(\frac{1}{\gamma}\right) \tag{25}$$

as well as at ultramicroelectrodes under steady state conditions ($\sigma << 1$), independently of the electrode geometry:

$$E_{\text{peak}}^{\text{SWV,UME}} = E_{\text{peak}}^{\text{DDPV,UME}} = E_{1/2}^{\text{UME}} = E_{\text{app}}^{0'} + \frac{RT}{F}\ln\left(\frac{1}{\gamma^2}\right) \tag{26}$$

On the other hand, at microelectrodes under transient conditions a significant discrepancy (>11 mV) between $E_{1/2}$ and the peak potential in SWV can be observed under the conditions of Figure 3. Therefore, one must be cautious in the identification of the value of the peak potential (in SWV and DDPV) with that of the half-wave potential when microelectrodes are employed and the effective diffusion coefficients are expected to differ. Moreover, Figure 3 shows that the experimental determination of the peak potential in SWV (or DDPV) with various pulse durations (*i.e.*, SW frequencies) and/or electrode radii enables us to extract the apparent formal potential (Eq.(13)) as well as the ratio between the effective diffusion coefficients (Eq.(10)) [28].

The influence of the pulse amplitude on the SWV (E_{SW}) and DDPV (ΔE) curves is analyzed in Figure 4. It is observed that the increase of E_{SW} and ΔE leads to higher peak currents whereas the peak potential remains unaffected. A broad *plateau* is obtained for very large pulse amplitudes in both techniques, the determination of the position of the voltammogram becoming less accurate under such conditions where capacitive effects are also likely to be very distorting. The current density of the *plateau* for SWV and $\gamma = 1$ at microspheres (Fig. 4B) coincides with the value predicted by [41]:

$$\frac{\Delta I_{\text{SWV}}^{\text{plateau}}}{I_{\text{d}}(\tau)} = 1.21 + \frac{\sqrt{\pi D\tau}}{r_0} \tag{27}$$

whereas the *plateau* current density corresponding to microdiscs (Fig. 4A) is slightly higher. This difference increases as r_0 shrinks in both techniques according to:

$$\text{macro} \;-\; \text{micro} \;-\; \text{UMEs}\ (r_s = r_d)$$

$$1 \;\le\; \frac{\Delta I_{peak}^{disc} / A_{disc}}{\Delta I_{peak}^{sph} / A_{sph}} \;\le\; \frac{4}{\pi} \qquad (28)$$

In the insets of Figure 4, the amplitude-normalized peak current [45] in SWV $\left(\Psi^{SWV} = \Delta I_{peak}^{SWV} / I_d(\tau) E_{SW}\right)$ and DDPV $\left(\psi^{DDPV} = \left|\Delta I_{peak}^{DDPV} / I_d(\tau_2)\Delta E\right|\right)$ is plotted *versus* the pulse amplitude. A monotonous decrease of Ψ^{SWV} and Ψ^{DDPV} with the pulse amplitude is observed, in contrast with the behaviour of quasi- or irreversible electron transfers where a maximum has been predicted [45]. This maximum is dependent on the degree of reversibility and, therefore, the study of the variation of the peak current with the amplitude allows for characterization the electrode kinetics.

Figure 5 shows the variation of the half-peak width ($W_{1/2}$) of the SWV and DDPV curves with the pulse amplitude (E_{SW} and ΔE), for spherical and disc microelectrodes under transient conditions. Grey solid lines correspond to the $W_{1/2}$-values predicted for any γ-value at macroelectrodes and under steady state conditions as well as for microelectrodes when $\gamma = 1$ [27]:

$$W_{1/2}^{j} = \frac{RT}{F} \ln\left[\frac{1 + e^{2\eta_j} + 4e^{\eta_j} + \sqrt{\left(1 + e^{2\eta_j} + 4e^{\eta_j}\right)^2 - 4e^{2\eta_j}}}{1 + e^{2\eta_j} + 4e^{\eta_j} - \sqrt{\left(1 + e^{2\eta_j} + 4e^{\eta_j}\right)^2 - 4e^{2\eta_j}}}\right];\ j \equiv \text{SWV,DDPV} \qquad (29)$$

with $\eta_{SW} = \frac{FE_{SW}}{RT}$ and $\eta_{DDPV} = \frac{F|\Delta E|}{2RT}$.

In all cases, $W_{1/2}$ increases with the pulse amplitude whatever the value of γ, the electrochemical technique and the electrode geometry. The latter is found to have a non-significant influence on $W_{1/2}$. Regarding the effect of γ, this is much more apparent in DDPV than in SWV where the value of $W_{1/2}^{SWV}$ is almost uniquely determined by E_{SW}. Thus, Eq. (29) applies reasonably well at microelectrodes with $\gamma \neq 1$, the deviations

being always smaller than 10 mV under the conditions considered in Figure 5A. This fact is very convenient since it enables us to use the experimental $W_{1/2}^{SWV}$-value as an indicator of deviations from full reversibility and/or the occurrence of ohmic drop effects almost independently of the electrode geometry, the SW frequency and the values of diffusion coefficients.

The effect of varying the staircase potential (E_s) on the SWV curve is analyzed in Figure 6 at macroelectrodes (Fig. 6A), spherical microelectrodes (Fig. 6B) and disc microelectrodes (Fig. 6C) for different values of γ. The position of the voltammograms is not affected by the value of E_s at macroelectrodes whereas the influence on the peak current is the same for any ratio D_{eff} / D'_{eff}. Thus, slightly larger values of ΔI_{peak} are found when E_s is increased (4.5% increase from $E_s = 2$ to $E_s = 10$). On the other hand, the variation of the peak height with E_s is a function of the γ-value at microelectrodes. As can be seen in Figures 6B and 6C, the influence on the peak current is qualitatively analogous for spherical and disc microelectrodes. Hence, the decrease of E_s leads to a higher SWV response when $\gamma > 1$ and the opposite is observed when $\gamma < 1$. The variation is negligible when $D_{eff} = D'_{eff}$ ($\gamma = 1$).

Cyclic square wave voltammograms at disc and spherical electrodes are shown in Figure 7 for different electrode sizes. At macro- (Fig.7A) and ultramicroelectrodes (Fig.7C) the peak heights for the forward ($E_S < 0$) and reverse ($E_S > 0$) scans are the same for any values of the diffusion coefficients (*i.e.*, any value of γ). However, at intermediate-size electrodes (Fig.7B) a different behaviour is observed for $\gamma \neq 1$ (*i.e.*, $D_{eff} \neq D'_{eff}$). Thus, the peak current in the normal scan is higher than that in the reverse one when $\gamma < 1$, whereas the opposite situation is observed when $\gamma > 1$. These results

are observed for any typical E_S-value (2-10 mV). Therefore, SWV curves in cyclic mode offer very easy detection of differences between species diffusivities from visual examination of the two peaks provided that medium-size microelectrodes are employed. Also, by fitting of experimental values of the forward and reverse peak currents and the peak position, the simultaneous determination of γ and $E_{\text{app}}^{0'}$ is possible.

Note that different magnitudes of the forward and reverse peaks are also predicted when the electrode process is not fully reversible [46]. These two situations (non-reversible electron transfer *vs* unequal diffusion coefficients) can be discriminated attending to the value of the half-peak width of the SWV peak that, as discussed above, is described with small error by Eq. (29) when the electrode reaction is reversible.

4. CONCLUSIONS

A theoretical study of square wave voltammetry (SWV) when the (effective) diffusion coefficients of the oxidized and reduced species are notably different ($D_{\text{eff}} \neq D'_{\text{eff}}$) has been performed, the results having been compared with those in differential double pulse voltammetry (DDPV).

At macroelectrodes and ultramicroelectrodes (steady-state conditions), when only the oxidized (or reduced) species are initially present the effect of unequal diffusion coefficients reduces to the shift of the peak potential with respect to the case $D_{\text{eff}} = D'_{\text{eff}}$, which coincides with the half-wave potential and it can be quantified with simple analytical expressions.

At microelectrodes under transient conditions, the occurrence of unequal diffusivities has more profound impact. Both the SWV peak position and peak magnitude are affected by the diffusion coefficient of the product of the electrode reaction (D'_{eff}): the larger the D'_{eff}-value, the smaller the peak height and the peak overpotential. Also, the influence of the experimental variables and technique parameters is unusual when $D_{\text{eff}} \neq D'_{\text{eff}}$, the peak potential varying with the duration of the potential pulses (*i.e.*, with the SW frequency) and with the microelectrode size. Moreover, a notable difference may exist between the half-wave potential and the peak potential.

All the above makes the rigorous, quantitative analysis of experimental SWV peaks more complex, the use of numerical simulations being required in most cases. As a “counterpart”, the simultaneous determination of the (effective) diffusion coefficients of the different species along with the (apparent) formal potential is feasible with only one microelectrode by fitting of the values of the peak current(s) and peak potential at different SW frequencies.

Acknowledgments

The authors greatly appreciate the financial support provided by the Ministerio de Economia y Competitividad (Project Number CTQ2012-36700, co-funded by European Regional Development Fund) and by the Fundación Séneca de la Región de Murcia under the III PCTRM 2011-2014 Programme (Project 18968/JLI/13). EL also thanks the funding received from the European Union Seventh Framework Programme-Marie Curie COFUND (FP7/2007-2013) under UMU Incoming Mobility Programme ACTion (U-IMPACT) Grant Agreement 267143.

FIGURES

Figure 1. Potential-time perturbation applied in **A)** cyclic square wave voltammetry (SWV) and **B)** differential double pulse voltammetry (DDPV) in normal and reverse modes (solid and dashed lines, respectively).

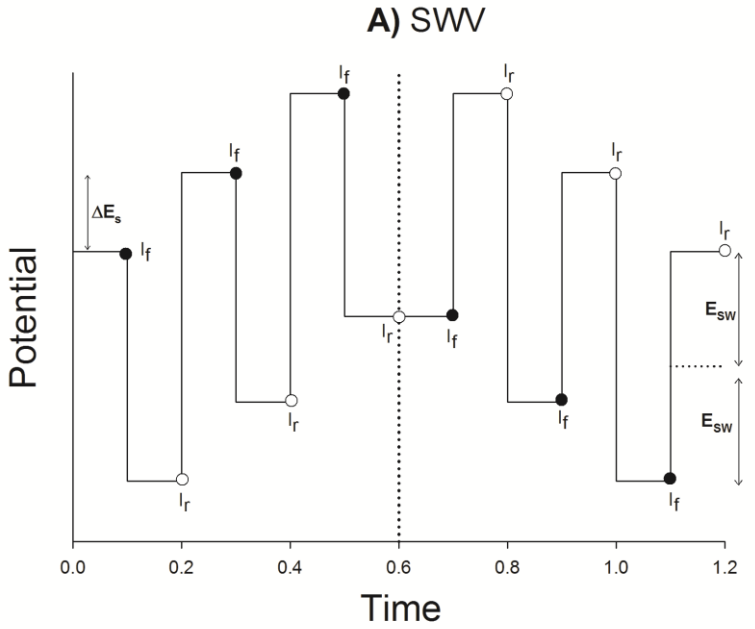

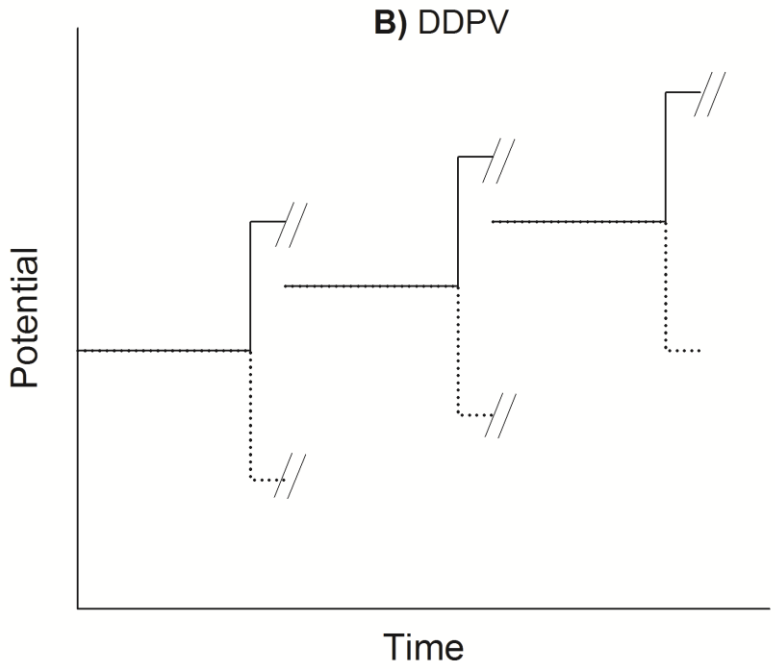

Figure 2. Influence of the ratio between the effective diffusion coefficients ($\gamma = \sqrt{D_{\text{eff}} / D'_{\text{eff}}}$) on the SWV and DDPV voltammograms for spherical and disc electrodes and different σ-values ($\sigma^{\text{SWV}} = r_0^2 / D_{\text{eff}}\tau$, $\sigma^{\text{DDPV}} = r_0^2 / D_{\text{eff}}\tau_2$). SWV: $E_S = -10\text{mV}$, $E_{SW} = 25\text{mV}$. DDPV: $\tau_1 / \tau_2 = 100$, $\Delta E = -50\text{mV}$, $D_{\text{eff}} = 10^{-5}$ cm^2 s^{-1}. $I_d(t) = FAc^*_{AT}\sqrt{D_{\text{eff}} / \pi t}$.

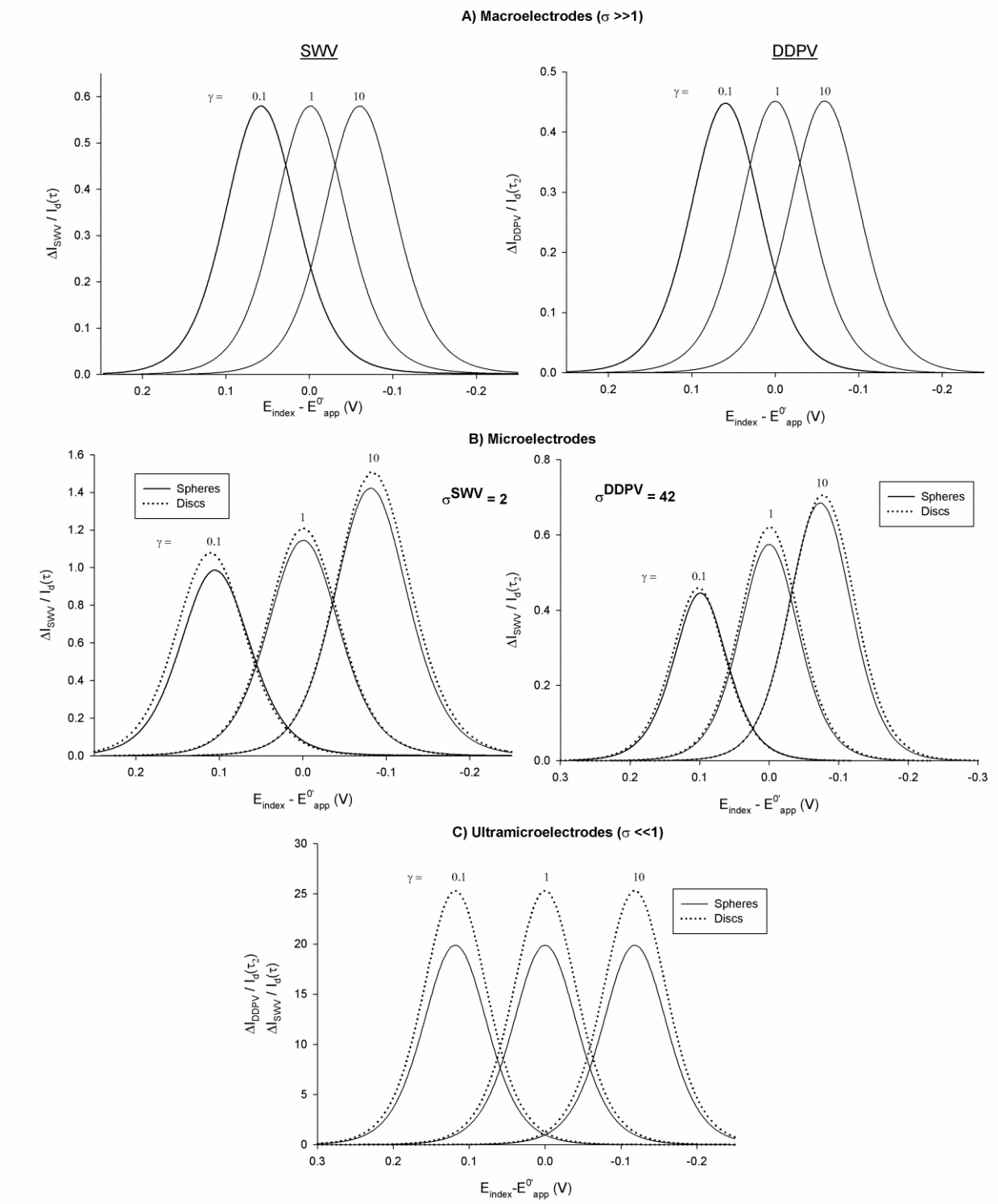

Fig. 3. Comparison between the variation of E_p^{DDPV}, E_p^{SWV}, and $E_{1/2}$ with σ ($\sigma^{SWV} = \sigma^{NPV} = r_0^2 / D_{eff}\tau$, $\sigma^{DDPV} = r_0^2 / D_{eff}\tau_2$) for different γ-values at **A)** spherical microelectrodes and **B)** disc microelectrodes.

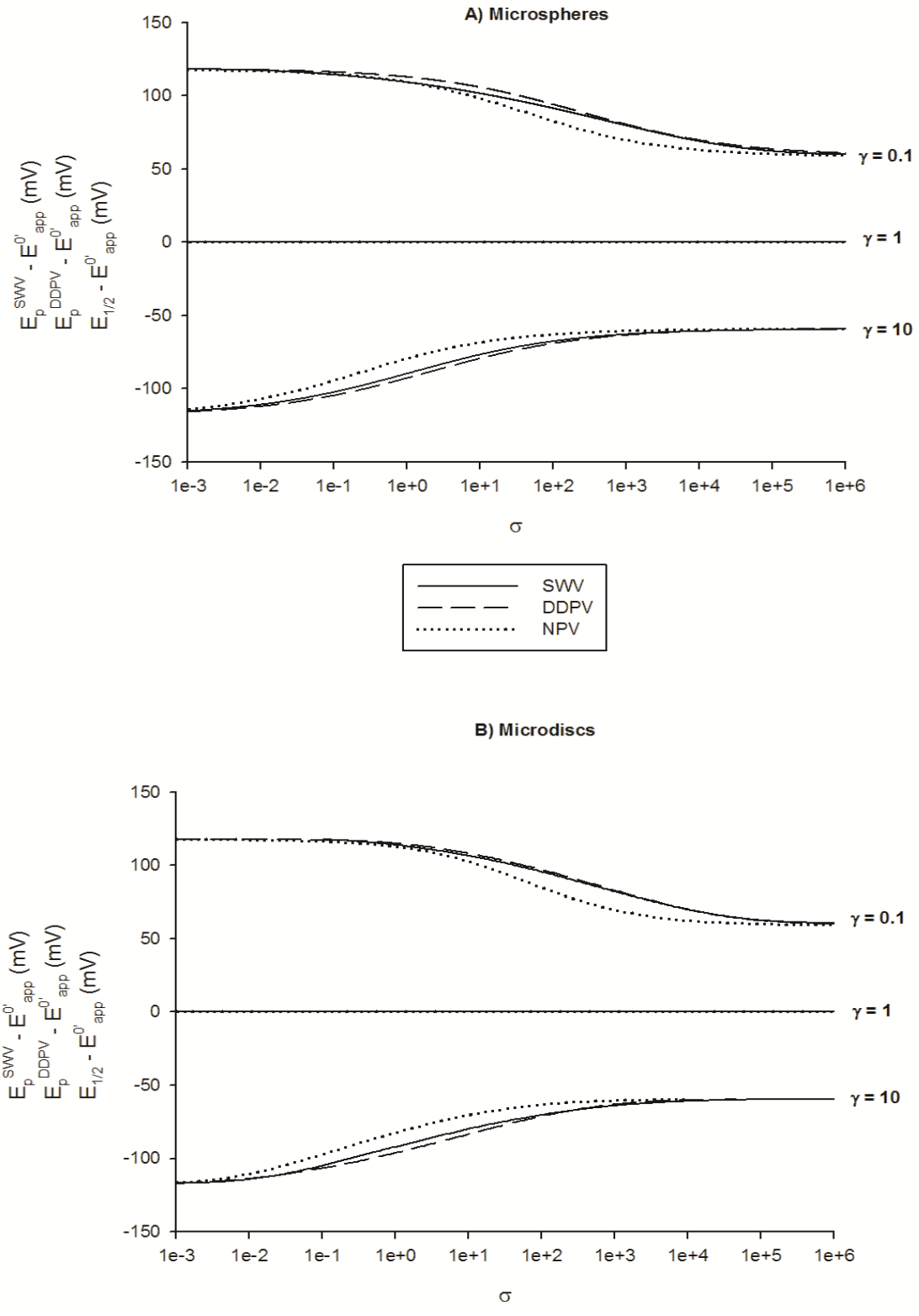

Fig. 4. SWV and DDPV voltammograms at spherical and disc microelectrodes for different pulse amplitude values and γ values. $D_{\text{eff}} = 10^{-5}\,\text{cm}^2\ \text{s}^{-1}$, $E_s = -5$ mV, $\tau_1 / \tau_2 = 100$, $\sigma = r_0^2 / D_{\text{eff}}\tau = r_0^2 / D_{\text{eff}}\tau_2 = 2$. *Insets*: variation of the amplitude normalized peak current in SWV ($\psi^{\text{SWV}} = \Delta I_{\text{peak}}^{\text{SWV}} / I_{\text{d}}(\tau) E_{\text{SW}}$) and DDPV ($\psi^{\text{DDPV}} = \left|\Delta I_{\text{peak}}^{\text{DDPV}} / I_{\text{d}}(\tau_2)\Delta E\right|$) with the pulse amplitude. $I_{\text{d}}(t) = FAc_{\text{AT}}^{*}\sqrt{D_{\text{eff}} / \pi t}$.

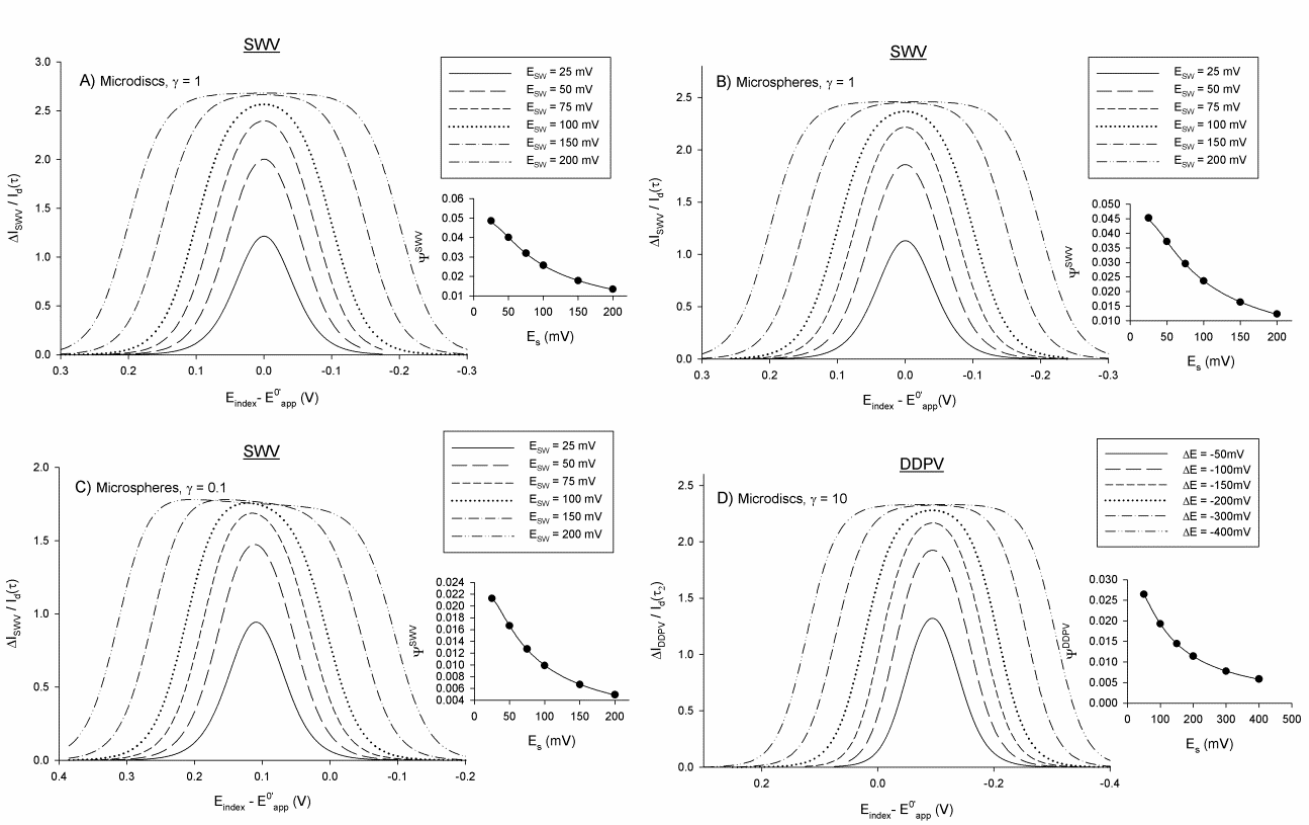

Fig. 5. Variation of the half-peak width ($W_{1/2}$) of SWV and DDPV voltammograms with the amplitude pulse at microspheres and microdiscs under transient conditions. **(A)** $\sigma = r_0^2 / D_{\text{eff}}\tau =$ 0.32 (for $\gamma = 10$) and 50.4 (for $\gamma = 0.1$); **(B)** $\sigma = r_0^2 / D_{\text{eff}}\tau_2 =$ 1.8 (for $\gamma = 10$) and 200 (for $\gamma = 0.1$). Values of γ indicated on the graphs.

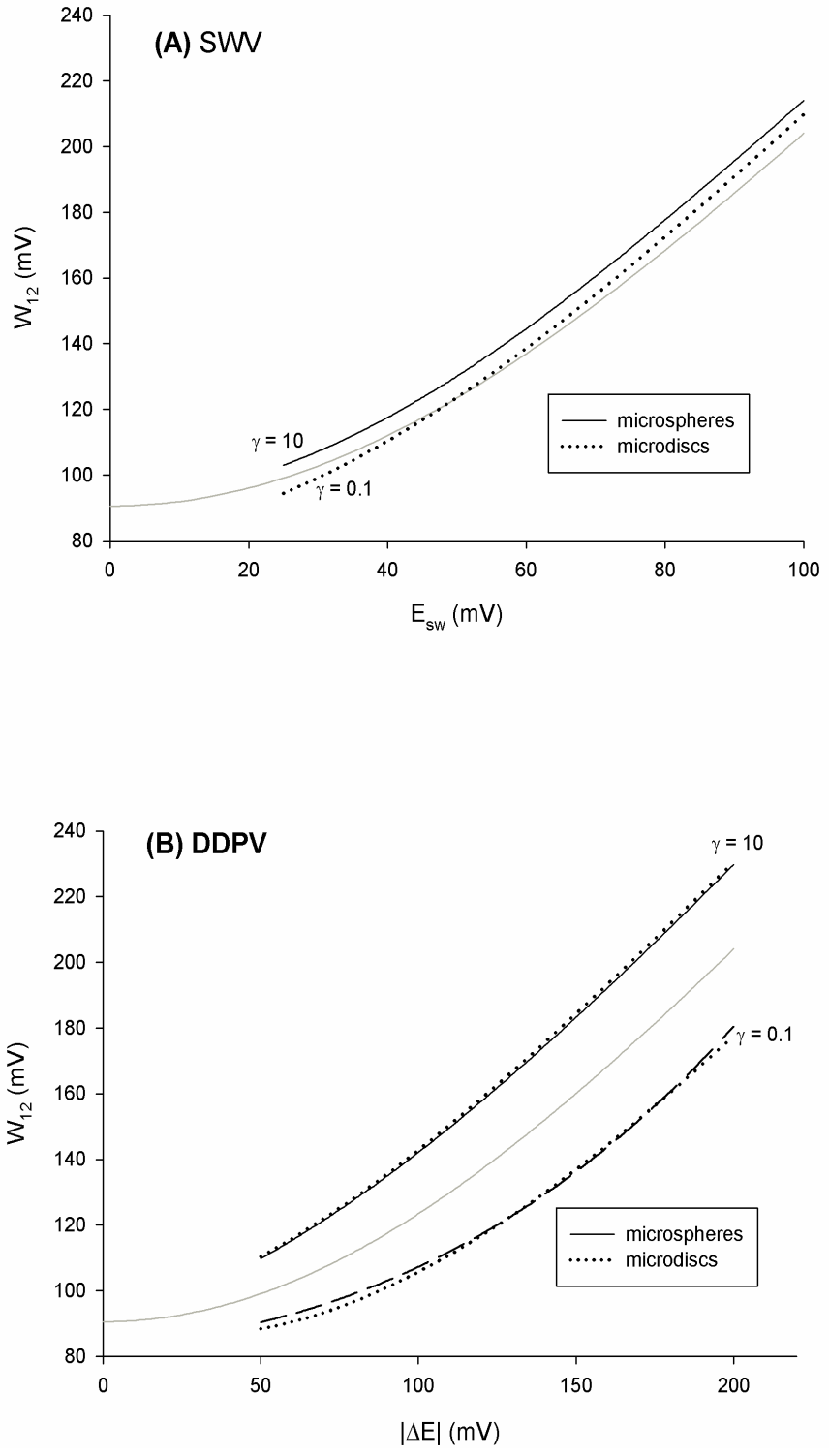

Fig. 6. Effect of the staircase potential (absolute value indicated on the graphs) on SWV at **A)** macroelectrodes, **B)** spherical microelectrodes and **C)** disc microelectrodes. $E_{\mathrm{SW}} = 25\mathrm{mV}$, $D_{\mathrm{eff}} = 10^{-5}\,\mathrm{cm^2\,s^{-1}}$, $\sigma^{\mathrm{SWV}} = r_0^2 / D_{\mathrm{eff}}\tau$. $I_{\mathrm{d}}(t) = FAc^*_{\mathrm{AT}}\sqrt{D_{\mathrm{eff}} / \pi t}$.

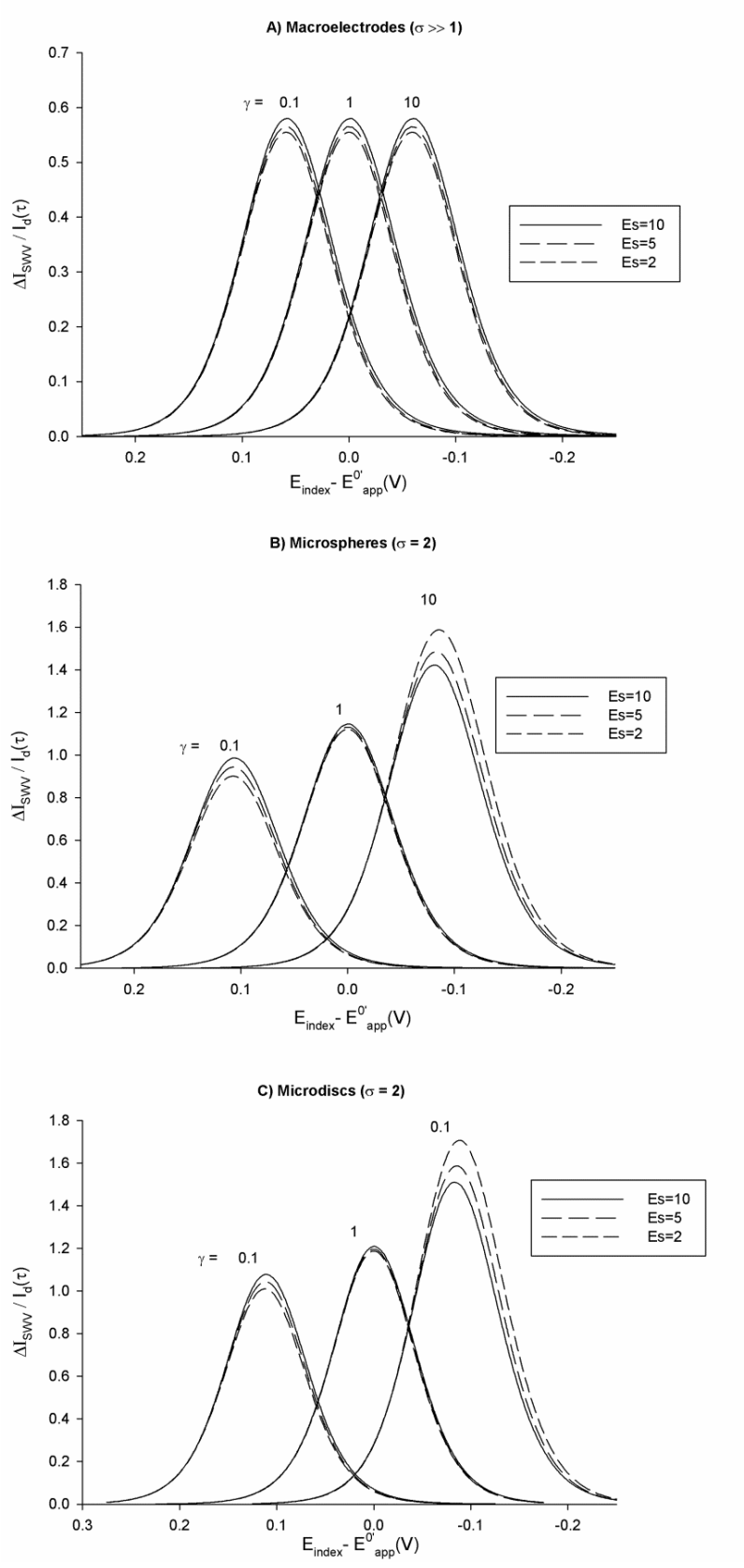

Fig. 7. Cyclic square wave voltammograms for spherical and disc **A)** macroelectrodes, **B)** microelectrodes and **C)** ultramicroelectrodes. $E_{\mathrm{SW}} = 25\mathrm{mV}$, $\left|E_s\right| = 10\,\mathrm{mV}$, $E_{\mathrm{p}} - E_{\mathrm{vertex}} = 200\,\mathrm{mV}$, $D_{\mathrm{eff}} = 10^{-5}\,\mathrm{cm}^2\ \mathrm{s}^{-1}$, $\sigma = r_0^2 / D_{\mathrm{eff}}\tau$, $I_{\mathrm{d}}(t) = FAc_{\mathrm{AT}}^{*}\sqrt{D_{\mathrm{eff}} / \pi\tau}$. The different values of γ are indicated on the graphs.

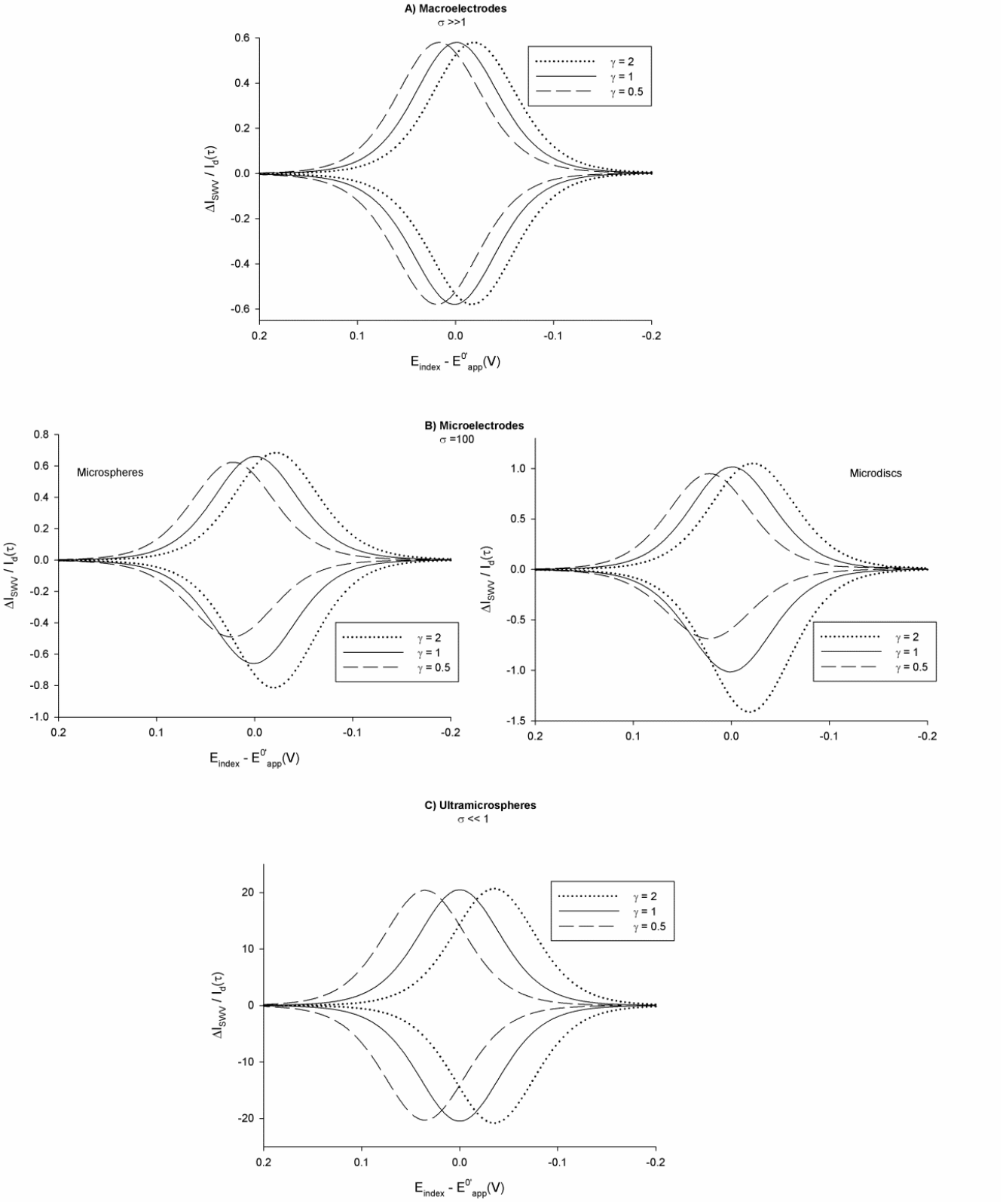

References

[1] A. De Rache, C. Buess-Herman, T. Doneux, Electrochemical square scheme analysis of macromolecule–electroactive ligand interactions, and its application to DNA binding, J. Electroanal. Chem., 745 (2015) 44-55.

[2] A. De Rache, T. Doneux, I. Kejnovská, C. Buess-Herman, On the interaction between [Ru (NH 3) 6] 3+ and the G-quadruplex forming thrombin binding aptamer sequence, J. Inorg. Biochem., 126 (2013) 84-90.

[3] T. Matsue, D.H. Evans, T. Osa, N. Kobayashi, Electron-transfer reactions associated with host-guest complexation. Oxidation of ferrocenecarboxylic acid in the presence of β-cyclodextrin, J. Am. Chem. Soc., 107 (1985) 3411-3417.

[4] D. Osella, A. Carretta, C. Nervi, M. Ravera, R. Gobetto, Inclusion complexes of ferrocenes and β-cyclodextrins. Critical appraisal of the electrochemical evaluation of formation constants, Organometallics, 19 (2000) 2791-2797.

[5] J.P. Pinheiro, R. Domingos, R. Lopez, R. Brayner, F. Fiévet, K. Wilkinson, Determination of diffusion coefficients of nanoparticles and humic substances using scanning stripping chronopotentiometry (SSCP), Colloids and Surfaces A: Physicochemical and Engineering Aspects, 295 (2007) 200-208.

[6] A. Vallat, M. Person, L. Roullier, E. Laviron, Electrochemical study of thermodynamics and kinetics of the cis-trans isomerization of dicarbonylbis [1, 2-bis (diphenylphosphino) ethane] molybdenum and-tungsten complexes and their cations, Inorg. Chem., 26 (1987) 332-335.

[7] C. Batchelor-McAuley, B.R. Kozub, D. Menshykau, R.G. Compton, Voltammetric Responses of Surface-Bound and Solution-Phase Anthraquinone Moieties in the Presence of Unbuffered Aqueous Media, J. Phys. Chem. C, 115 (2010) 714-718.

[8] E. Laviron, Electrochemical reactions with protonations at equilibrium: Part X. The kinetics of the p-benzoquinone/hydroquinone couple on a platinum electrode, J. Electroanal. Chem., 164 (1984) 213-227.

[9] E. Laborda, J.M. Olmos, E. Torralba, A. Molina, Application of Voltammetric Techniques at Microelectrodes to the Study of the Chemical Stability of Highly Reactive Species, Anal. Chem., 87 (2015) 1676-1684.

[10] N.A. Macías-Ruvalcaba, D.H. Evans, Study of the effects of ion pairing and activity coefficients on the separation in standard potentials for two-step reduction of dinitroaromatics, J. Phys. Chem. B, 109 (2005) 1464214647.

[11] J. Galceran, J. Puy, J. Salvador, J. Cecília, H.P. van Leeuwen, Voltammetric lability of metal complexes at spherical microelectrodes with various radii, J. Electroanal. Chem., 505 (2001) 85-94.

[12] H.P. van Leeuwen, J.-P. Pinheiro, Lability criteria for metal complexes in micro-electrode voltammetry, J. Electroanal. Chem., 471 (1999) 55-61.

[13] A. Molina, C. Serna, J.A. Ortuño, E. Torralba, Studies of ion transfer across liquid membranes by electrochemical techniques, Annu. Rep. Prog. Chem. Sect. C, 108 (2012) 126-176.

[14] A. Molina, E. Torralba, C. Serna, J.A. Ortuño, Analytical solution for the facilitated ion transfer at the interface between two inmiscible electrolyte solutions via successive complexation reactions in any voltammetric technique. Application to Square Wave Voltammetry and Cyclic Voltammetry, Electrochim. Acta, 106 (2013) 244-257.

[15] M.C. Osborne, Y. Shao, C.M. Pereira, H.H. Girault, Micro-hole interface for the amperometric determination of ionic species in aqueous solutions, J. Electroanal. Chem., 364 (1994) 155-161.

[16] M. Sairi, J. Strutwolf, R.A. Mitchell, D.S. Silvester, D.W. Arrigan, Chronoamperometric response at nanoscale liquid–liquid interface arrays, Electrochim. Acta, 101 (2013) 177-185.

[17] E. Torralba, J.A. Ortuño, A. Molina, C. Serna, F. Karimian, Facilitated ion transfer of protonated primary organic amines studied by square wave voltammetry and chronoamperometry, Anal. Chim. Acta, 826 (2014) 12-20.

[18] M.C. Buzzeo, O.V. Klymenko, J.D. Wadhawan, C. Hardacre, K.R. Seddon, R.G. Compton, Voltammetry of oxygen in the room-temperature ionic liquids 1-ethyl-3-methylimidazolium bis ((trifluoromethyl) sulfonyl) imide and hexyltriethylammonium bis ((trifluoromethyl) sulfonyl) imide: one-electron reduction to form superoxide. Steady-state and transient behavior in the same cyclic voltammogram resulting from widely different diffusion coefficients of oxygen and superoxide, J. Phys. Chem. A, 107 (2003) 8872-8878.

[19] R.G. Evans, O.V. Klymenko, P.D. Price, S.G. Davies, C. Hardacre, R.G. Compton, A comparative electrochemical study of diffusion in room temperature ionic liquid solvents versus acetonitrile, ChemPhysChem, 6 (2005) 526-533.

[20] J. Ghilane, C. Lagrost, P. Hapiot, Scanning electrochemical microscopy in nonusual solvents: inequality of diffusion coefficients problem, Anal. Chem., 79 (2007) 7383-7391.

[21] D. Zigah, J. Ghilane, C. Lagrost, P. Hapiot, Variations of diffusion coefficients of redox active molecules in room temperature ionic liquids upon electron transfer, J. Phys. Chem. B, 112 (2008) 14952-14958.

[22] A.J. Bard, L.R. Faulkner, Electrochemical Methods, 2nd ed., Wiley, New York, 2001.

[23] D.P. Whelan, J.J. O'Dea, J. Osteryoung, K. Aoki, Square wave voltammetry at small disk electrodes: Theory and experiment, J. Electroanal. Chem., 202 (1986) 23-36.

[24] Š. Komorsky-Lovrić, M. Lovrić, A. Bond, Square-wave voltammetry at spherical and disk microelectrodes as a function of electrode radius and frequency, Electroanalysis, 5 (1993) 29-40.

[25] D.E. Tallman, Square wave voltammetry of reversible systems at ring microelectrodes. 1. Theoretical study, Anal. Chem., 66 (1994) 557-565.

[26] V. Mirčeski, Š. Komorsky-Lovrić, M. Lovrić, Square-Wave Voltammetry, Theory and Application, Springer, Heidelberg, 2007.

[27] A. Molina, J. Gonzalez, E. Laborda, R. Compton, Mass transport at electrodes of arbitrary geometry. Reversible charge transfer reactions in square wave voltammetry, Russ. J. Electrochem., 48 (2012) 600-609.

[28] E. Laborda, J.M. Olmos, F. Martínez-Ortiz, A. Molina, Voltammetric speciation studies of systems where the species diffusivities differ significantly, J. Solid State Electrochem., 19 (2015) 549-561.

[29] Á. Molina, E. Laborda, E.I. Rogers, F. Martínez-Ortiz, C. Serna, J.G. Limon-Petersen, N.V. Rees, R.G. Compton, Theoretical and experimental study of Differential Pulse Voltammetry at spherical electrodes: Measuring diffusion coefficients and formal potentials, J. Electroanal. Chem., 634 (2009) 73-81.

[30] O.V. Klymenko, R.G. Evans, C. Hardacre, I.B. Svir, R.G. Compton, Double potential step chronoamperometry at microdisk electrodes: simulating the case of unequal diffusion coefficients, J. Electroanal. Chem., 571 (2004) 211-221.

[31] E. Laborda, E.I. Rogers, F. Martínez-Ortiz, J.G. Limon-Petersen, N.V. Rees, Á. Molina, R.G. Compton, Reverse Pulse Voltammetry at spherical electrodes: Simultaneous determination of diffusion coefficients and formal potentials. Application to Room Temperature Ionic Liquids, J. Electroanal. Chem., 634 (2009) 1-10.

[32] A. Molina, R.G. Compton, C. Serna, F. Martínez-Ortiz, E. Laborda, Theory for Double Potential Step Chronoamperometry for any potential values at spherical electrodes. Simultaneous determination of the diffusion coefficients of the electroctive species., Electrochim. Acta, 54 (2009) 2320-2328.

[33] A. Molina, J.M. Olmos, E. Laborda, Reverse Pulse Voltammetry at Spherical and Disc Microelectrodes: Characterization of Homogeneous Chemical Equilibria and Their Impact on the Species Diffusivities, Electrochim. Acta, 169 (2015) 300-309.

[34] Y. Wang, J.G. Limon-Petersen, R.G. Compton, Measurement of the diffusion coefficients of $[Ru(NH_3)_6]^{3+}$ and $[Ru(NH_3)_6]^{2+}$ in aqueous solution using microelectrode double potential step chronoamperometry, J. Electroanal. Chem., 652 (2011) 13-17.

[35] Y. Wang, E.I. Rogers, R.G. Compton, The measurement of the diffusion coefficients of ferrocene and ferrocenium and their temperature dependence in acetonitrile using double potential step microdisk electrode chronoamperometry, J. Electroanal. Chem., 648 (2010) 15-19.

[36] E. Laborda, J.M. Olmos, A. Molina, Differential double pulse voltammetry at spherical microelectrodes for the characterization of the square mechanism, J. Electroanal. Chem., 741 (2015) 140-148.

[37] J. Janisch, A. Ruff, B. Speiser, C. Wolff, J. Zigelli, S. Benthin, V. Feldmann, H.A. Mayer, Consistent diffusion coefficients of ferrocene in some non-aqueous solvents: Electrochemical simultaneous determination together with electrode sizes and comparison to pulse-gradient spin-echo NMR results, J. Solid State Electrochem., 15 (2011) 2083-2094.

[38] I. Reche, I. Gallardo, G. Guirado, Cyclic voltammetry using silver as cathode material: a simple method for determining electro and chemical features and solubility values of CO 2 in ionic liquids, Phys. Chem. Chem. Phys., 17 (2015) 2339-2343.

[39] K.B. Oldham, Errors arising from carrying out integration, and other operations of calculus, on digitally acquired data, J. Electroanal. Chem., 208 (1986) 1-12.

[40] J. Crank, The Mathematics of Diffusion, 2nd ed., Oxford Science Publications, 1975.

[41] A. Molina, M.M. Moreno, C. Serna, M. López-Tenés, J. González, N. Abenza, Study of multicenter redox molecules with square wave voltammetry, J. Phys. Chem. C, 111 (2007) 12446-12453.

[42] K.B. Oldham, C.G. Zoski, Comparison of voltammetric steady states at hemispherical and disc microelectrodes, J. Electroanal. Chem., 256 (1988) 11-19.

[43] F. Martínez-Ortiz, N. Zoroa, A. Molina, C. Serna, E. Laborda,Electrochemical digital simulation with an exponential expanding grid: general expresions for higher order approximations to spatial derivatives. The special case of four point formulas and their application to multipulse techniques in planar and any size spherical electrodes Electrochim. Acta, 54 (2009) 1042-1055.

[44] R.G. Compton, E. Laborda, K.R. Ward, Understanding Voltammetry: Simulation of Electrode Processes, World Scientific, Singapore, 2014.

[45] V. Mirceski, E. Laborda, D. Guziejewski, R.G. Compton, New approach to electrode kinetic measurements in square-wave voltammetry: amplitude-based quasireversible maximum, Anal. Chem., 85 (2013) 5586-5594.

[46] M.A. Mann, J.C. Helfrick Jr, L.A. Bottomley, Diagnostic Criteria for the Characterization of Quasireversible Electron Transfer Reactions by Cyclic Square Wave Voltammetry, Anal. Chem., 86 (2014) 8183-8191.